Measurements and Modeling of Impulse Noise at the 2.4 GHz Wireless LAN Band

Khodr A. Saaifan and Werner Henkel
Jacobs University Bremen, Bremen 28759, Germany
{k.saaifan, w.henkel}@jacobs-university.de

***Abstract*—Radio frequency interference (RFI) of industrial, scientific, and medical (ISM) equipment at 2.4 GHz can corrupt a wireless communication channel that shares the same band. Interference modeling of ISM radio emissions leads to a Middleton Class-A (MCA) model, which represents the impacts of additive white Gaussian noise (AWGN) superimposed to impulsive emissions of ISM interference. The statistical-physical extension of the MCA model for multiple receive antennas has so far been limited to two antennas. Herewith, we provide a measurement campaign at a 2.4 GHz band to capture the impulsive interference caused by various ISM sources. To verify a multivariate extension of the MCA model for multiple receive antennas, the measurement campaign implemented 4 receive antennas. This allows us to investigate the spatial coupling and correlation of measured interference in contrast to the multivariate MCA model.**

***Keywords*—RF interference, impulse noise, measurements, multiple antennas**

I. Introduction

The 2.4 GHz industrial, scientific, and medical (ISM) band is originally reserved for the use of radio frequency (RF) radiation and emissions of ISM equipment such as microwave ovens, medical equipment, car ignition, and hairdryers. The radio transmission technologies in the 2.4-GHz band such as Bluetooth, cordless phones, and wireless local area networks are subject to strong interference caused by ISM appliances. Interference measurements at the 2.4 GHz band [1]–[3] show that the ISM interference exhibits the impulsive nature of a Middleton Class-A (MCA) model [4]. The MCA model is designated by two parameters to fit a wide variety of impulse noise environments occurring in practice. For multi-antenna systems, the MCA model already comes with question marks, almost no correlation (memoryless) properties, neither in time nor in space, except for rudimentary 2-antenna systems [5]. The statistical-physical extension of this model to an arbitrary number of receive antennas is complicated, which restricts a receiver design problem to two receive antennas.

In this paper, we provided multi-antenna measurements of impulse noise at a 2.4 GHz wireless LAN band. We analytically relate the properties of measured impulses to the parameters of the MCA model. Furthermore, we extend and verify the MCA model to represent the multi-antenna measurements. Thus, we adopt a correlated multivariate MCA model to describe the spatial coupling of impulse noise. The rest of the paper is organized as follows. Section II introduces impulse noise measurements (setup and results) of ISM interference at the 2.4 GHz band. In Section III, we describe the MCA model and its extension to represent impulse noise for multi-antenna systems. Section IV verifies the MCA model for representing the impacts of ISM interference inside a wireless LAN spectrum. Finally, concluding remarks are presented in Section V.

II. Impulse Noise Measurements

In this section, we introduced a measurement campaign to measure impulse noise at the 2.4 GHz band for multi-antenna systems. We looked into the interference caused by industrial and other impulse-noise sources such as car ignition and electrical drills.

A. Measurements Setup

The measurement setup consists of an RF receiver, a digital oscilloscope, a network analyzer, and a laptop. Figure 1 illustrates the measurement step for impulse noise at the 2.4 GHz band. The receiver consists of four antenna elements, a

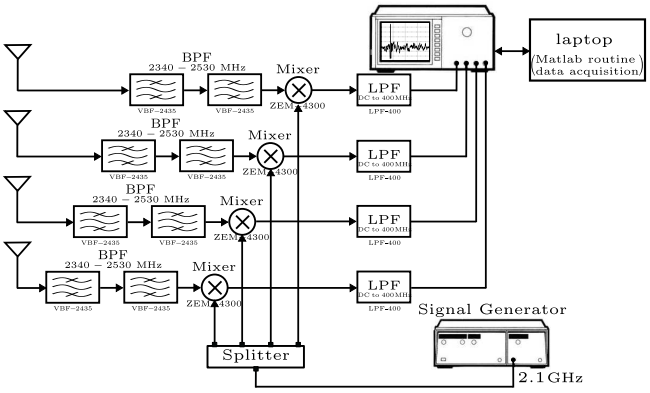

Fig. 1: The impulse noise measurement setup

bank of bandpass filters (centered at $f_c = 2.435$ GHz), and downconversion mixers. The antenna elements are mounted on a conducting steel sheet with adjustable antenna spacing[1]. We used a quarter-wave monopole antenna designed at the center frequency $f_c = 2.4$ GHz. The bandpass filters pass the signals within a wireless LAN range, i.e., the range of 2.340-2.530 GHz. The 6 dB RF bandwidth of the BPF is 190 MHz, which determines the bandwidth of the receiver, W_s. The signals from the filters are mixed down with a carrier from a local oscillator (LO). The frequency of the LO signal

[1]The distance between the adjacent elements is approximately equal to $\lambda/4$.

was selected such that the intermediate frequency, $f_{IF} = 300$ MHz, of the output signals are within the frequency range of the oscilloscope, i.e., we chose the LO carrier to be $f_{LO} = 2.1$ GHz for a digital oscilloscope with a 400 MHz bandwidth. We use a Matlab program to acquire and transfer the measurement data from the oscilloscope to a controlling laptop.

The measurements were originally sampled by the oscilloscope with a sampling rate of 5 GHz. However, the stored data are further downsampled (by a factor of 4) to decrease the size of measured data. The sampling interval is given by $T_s = 0.8\,ns$. The measured waveforms are stored in segments of duration $0.2\,\mu$s (250 samples per segment[2]). The program only stores segments with impulse noise since the oscilloscope is window-triggered to capture the impulsive events. In each acquisition, we stored a block of 1000 segments as well as the triggering time of each segment. The measurements were repeated to collect sufficient data (we collected 100 blocks for each measurement) to analyze the statistical characteristics of impulse noise.

B. Measurement Results

Figures 2, 3, and 4 depict multi-antenna measurements for impulse noise caused by car ignition, manufacturing car electronic components, and shoe production equipment, respectively. We note that the impulsive interference $w_I(t)$ after

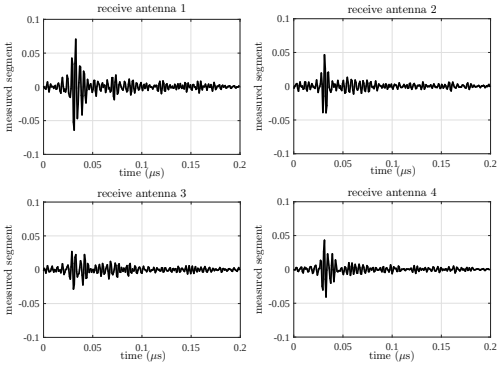

Fig. 2: Interference at the four receive antennas caused by car ignition

filtering and calibration is active only for a short duration T_I, which depends on the type of impulse noise. The results indicate two interesting properties of impulse noise inside the 2.4 GHz band. First, we observe that the impulsive components of interference consist of very short random impulses. Second, the impacts of impulse noise at the four receiving antennas appeared jointly, which is consistent with the spatial coupling of a bivariate MCA model for 2 receive antennas [5], [6].

III. Impulse Noise Models

In this section, we involve measured data to enhance the understanding of the parameters of the MCA model. Additionally, we introduce a multivariate MCA model to extend MCA modeling for multiple receive antennas.

[2]Parameters can be modified and had to be adjusted depending on the local impulse noise conditions.

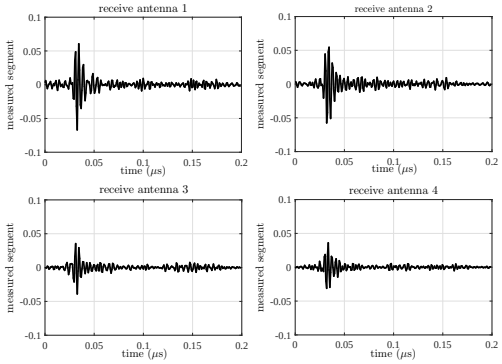

Fig. 3: Interference at the four receive antennas caused by manufacturing automotive components

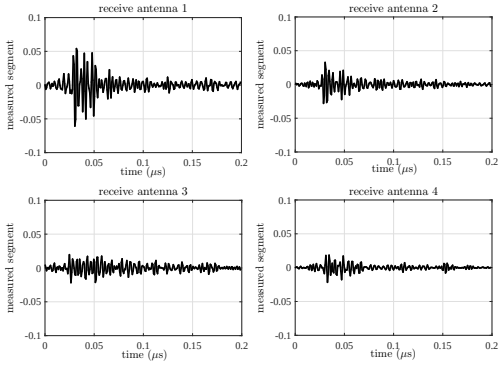

Fig. 4: Interference at the four receive antennas caused by a shoe production machine

A. The MCA Model

The MCA model [4] provides the amplitude distribution of the received interference at the IF stage of the receiver. Similar to measured interference at the 2.4 GHz band, the MCA model assumes that the received interference, $w(t)$, consists of two independent components: a Gaussian component, $w_G(t)$, and an interference component, $w_I(t)$. The Gaussian component represents AWGN with zero mean and variance σ_G^2. The interference component $w_I(t)$ consists of the emissions for an infinite number of interference sources. During the emission times of sources, the interference remains active for a certain duration T_I. However, the envelopes, frequencies, and phases of interference signals are randomly distributed. The source locations and emissions are distributed in space and time according to a homogeneous Poisson point process [4]. In fact, the homogeneous Poisson process is characterized by a constant parameter λ, which can be interpreted as the average number of source emissions per second. The number of emissions M corrupting an observation period T_P is given by a Poisson distribution as

$$P(M_{T_P} = M) = \frac{(\lambda T_P)^M \mathrm{e}^{-\lambda T_P}}{M!}\,, \qquad (1)$$

where λ denotes the average rate of impulses. The times between the impulses in a Poisson process are independent, exponentially distributed random variables. Accordingly, $T = 1/\lambda$ denotes the average period of impulses. We consider that the received interference $w(t)$ is sampled uniformly at times $t_k = k\Delta t$, $k = 1, 2, \ldots$, where $\Delta t < T_I$ is the sample spacing. The interference samples $w_k = w(k\Delta t)$ can be modeled by an MCA distribution as [4], [7]

$$p_w(w_k) = \sum_{m=0}^{\infty} \frac{\alpha_m}{\sqrt{2\pi\sigma_m^2}} \mathrm{e}^{-w_k^2/2\sigma_m^2} , \tag{2}$$

where (1) is used to determine the probability of having impulses α_m during a duration $T_P = T_I$ as

$$\alpha_m = \frac{A^m \mathrm{e}^{-A}}{m!} , \quad m = 0, 1, \ldots \infty , \tag{3}$$

and $A = \lambda T_I$ is the impulsive index of the MCA model. The terms $m = 0, 1, \ldots \infty$, are recognized as noise state information of the MCA model such as $m = 0$ denotes a Gaussian state and $m \geq 1$ represents the impulsive states. In each state, the MCA model assumes that the noise sample $w_k = w_G(t_k) + w_I(t_k)$ is a Gaussian random variable with zero mean and variance [8]

$$\sigma_m^2 = \sigma_G^2 + \frac{m}{A}\sigma_I^2 , \quad m = 0, 1, \ldots \infty , \tag{4}$$

where σ_G^2 denotes the variance of $w_G(t_k)$ and σ_I^2 is the variance of the interference component $w_I(t_k)$. The ratio, $\Upsilon = \sigma_G^2/\sigma_I^2$, represents the Gaussian factor of the MCA model. Typically, the value of Υ determines the power ratio of AWGN to the impulsive interference. Numerically, the impulsive index $A = \lambda T_I$ can take on any real positive value. However, Middleton limits the values of A to a specific range, $A \in [10^{-6}, 1]$, which can fit a wide variety of impulse noise environments. Since $A \leq 1$, the emission period $T = 1/\lambda$ is greater than the emission duration T_I, which resorts the impulsive behavior of the MCA model as illustrated in Fig. 5. Under the cyclostationarity assumption, the noise variance σ_I^2

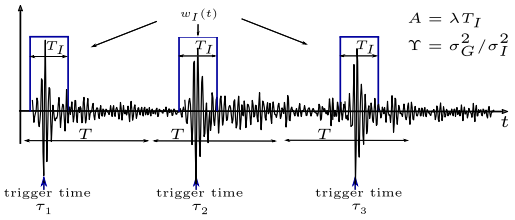

Fig. 5: The impulsive appearance of measured interference

can be related to the measured impulses $w_I(t)$ as

$$\sigma_I^2 = \frac{1}{T}\int_0^{T_I} |w_I(t)|^2 dt . \tag{5}$$

For $A \ll 1$, the impulsive index $A = T_I/T$ can be seen a duty cycle of the received impulses, and hence, the MCA model can be approximated by

$$p_w(w_k) = \frac{1-A}{\sqrt{2\pi\sigma_0^2}} \mathrm{e}^{-w_k^2/2\sigma_0^2} + \frac{A}{\sqrt{2\pi\sigma_1^2}} \mathrm{e}^{-w_k^2/2\sigma_1^2} . \tag{6}$$

which denotes a Gaussian mixture (GM) model [9], [10] of MCA noise.

B. The Multivariate MCA Model

The statistical-physical extension of the MCA model is limited to 2 receive antennas [5]. Since the MCA model for an arbitrary number of receive antennas is difficult, we adopt an algebraic extension as follows [11]:

$$p_{\mathbf{w}}(\mathbf{w}) = \sum_{m=0}^{\infty} \frac{\alpha_m}{(2\pi)^{\frac{N_R}{2}} |\mathbf{\Sigma}_m|^{\frac{1}{2}}} \mathrm{e}^{-\frac{1}{2}\mathbf{w}^T \mathbf{\Sigma}_m^{-1} \mathbf{w}} , \tag{7}$$

where $\mathbf{w} = [w_1, w_2, \cdots, w_{N_R}]^T$ is the spatial observation vector. Similar to the MCA model, we assume that the received interference w_{n_R}, $\forall n_R$, consist of two components w_{G,n_R} and w_{I,n_R}. The covariance matrix of interference $\mathbf{\Sigma}_m$ can be expressed as

$$\mathbf{\Sigma}_m = \begin{pmatrix} \sigma_{m,1}^2 & \cdots & \rho_{m,1N_R}\sigma_{m,1}\sigma_{m,N_R} \\ \vdots & \ddots & \vdots \\ \rho_{m,N_R1}\sigma_{m,N_R}\sigma_{m,1} & \cdots & \sigma_{m,N_R}^2 \end{pmatrix} , \tag{8}$$

where $\rho_{m,n_R\grave{n}_R}$ denotes the correlation coefficient of noise observations between the n_R^{th} and the $\grave{n}_R^{\text{th}}$ receive antenna for the m^{th} noise state. The variances of each state m can be rewritten as

$$\sigma_{m,n_R}^2 = \sigma_{G,n_R}^2 + \frac{m}{A}\sigma_{I,n_R}^2 = \sigma_{G,n_R}^2 \left(1 + \frac{m}{A\Upsilon_{n_R}}\right) , \tag{9}$$

where $\Upsilon_{n_R} = \sigma_{G,n_R}^2/\sigma_{I,n_R}^2$, $\forall n_R$, are the Gaussian factors of the multivariate MCA model. For $A \ll 1$, the first two terms $m = 0, 1$ are sufficient to approximate the joint PDF in (7). Thus, the correlation coefficients $\rho_{0,n_R\grave{n}_R} = \rho_{G,n_R\grave{n}_R}$ and $\rho_{1,n_R\grave{n}_R} = \rho_{I,n_R\grave{n}_R}$ determine the spatial correlations for background noise and impulsive interference, respectively.

IV. Model Verification

A. Amplitude Distributions

We examined the measured interference for different measurements to investigate the properties of impulse noise at 2.4 GHz. We used the triggering times of measured segments to compute the impulse rate λ. We also considered the impulse duration, T_I, and the impulse energy, $E_I = \int_0^{T_I} w_I(t)dt$, of measured data to calculate the parameters of the MCA model. In Table I, we provide the results of our measurements for car ignition and industrial settings, respectively. Since

TABLE I: The properties of measured impulse noise at 2.4 GHz

Measurements	T_I (μs)	λ	$A = \lambda T_I$	E_I (W/Hz)
car ignition	0.016	4	0.64×10^{-7}	1.4×10^{-11}
Automotive	0.01	8.3	0.83×10^{-7}	1.1×10^{-11}
shoe machines	0.018	99000	0.0018	4×10^{-11}

$A \leq 1$ for our measurements, we used a 2-term MCA model given in (6) to fit the PDF of measured interference. We use λ and E_I to compute the variance of impulsive

interference (5) Thus, the variances σ_m^2, $m = 0, 1$, can be rewritten as $\sigma_m^2 = \sigma_G^2 + \frac{m}{T_I} E_I$. We also made use of the Gaussian component, $w_G(t)$, of measured data to compute the variance of the Gaussian noise σ_G^2. Figure 6 illustrates the probability density function (PDF) for interference caused by car ignition, automobile component manufacturing, and a shoe machine, respectively. We also depict the MCA model with the corresponding modeling parameters deduced from the properties of measured interference.

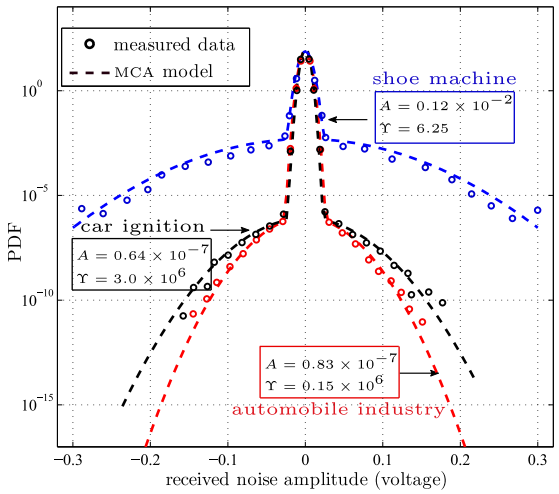

Fig. 6: The PDF of the measured interference compared with the MCA model

B. Spatial Coupling

Similar to the previous analysis, we investigate the properties of impulse noise measured at the four antennas after filtering and calibration as given in Table II. We limit the results to the multi-antenna measurements of a shoe production machine. We observe that the impulse energy, E_{I,n_R}, at the

TABLE II: The properties of impulse noise caused by a shoe production machine at 2.4 GHz for 4-receive antennas

measurements	T_I (μs)	λ	A	E_{I,n_R} (W/Hz)
antenna 1	≈ 0.018	99000	0.0018	4.0×10^{-11}
antenna 2				1.4×10^{-11}
antenna 3				1.5×10^{-11}
antenna 4				5.5×10^{-12}

four receive antennas, has different values. Similar to a single antenna, the variance, σ_{m,n_R}^2, $n_R = 1, \ldots, 4$, of the multivariate MCA model can be given as $\sigma_{m,n_R}^2 = \sigma_{G,n_R}^2 + \frac{m}{T_I} E_{I,n_R}$. In Fig. 7, we depict the voltage histograms of the measured interference at the four antennas. The figure also depicts the MCA model for the four antennas with the corresponding parameters A and Υ_{n_R} for multi-antenna measurements. Herewith, we also express Υ_{n_R} as the ratio $\sigma_{G,n_R}^2/\sigma_{I,n_R}^2$. To verify the spatial coupling of impulse noise, we compute the correlation coefficients of the measured segments between the receive antennas. Table III lists the spatial correlations of the measured impulse noise between the different receive

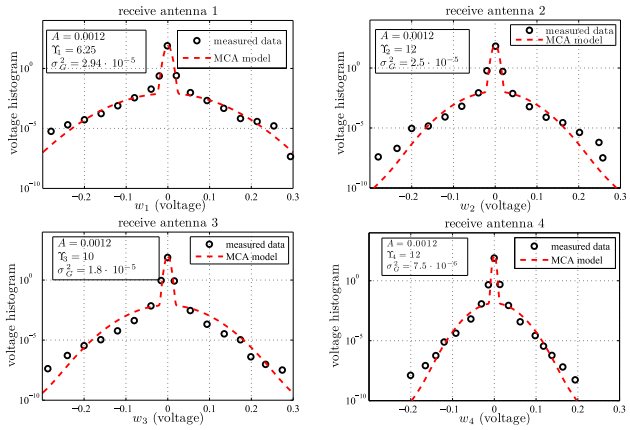

Fig. 7: The multivariate MCA model of measured interference caused by a shoe production machine

TABLE III: Spatial correlation of measured impulse noise

Measurements	$\rho_{m,12}$	$\rho_{m,13}$	$\rho_{m,14}$
Gaussian components, $m = 0$	0.1285	0.0154	0.1120
Impulsive components, $m = 1$	0.6708	0.3093	0.1755

antennas. We observe that the correlation coefficients of the Gaussian components, $\rho_{G,1,n_R}$, $\forall n_R$, are less than those of the impulse components, $\rho_{I,1,n_R}$. This was expected, since the receive antennas are typically affected by impulse noise caused by the same interference sources.

V. Conclusion

In this paper, we provided results from a measurement campaign to verify the Middleton Class-A (MCA) modeling for wireless interference at 2.4 GHz. We investigated the MCA extension to model impulse noise for multi-antenna systems. Using measurements, we showed that the MCA distribution fits well to the voltage histograms of the measured data. In particular, we noted that a 2-term MCA model is sufficient to capture the impulsive behavior of 2.4 GHz wireless interference. For multi-antenna systems, we verified a correlated multivariate MCA distribution to model the spatial coupling and dependency of impulse noise between the receive antennas. The measurements showed that the multi-antenna interferences have different variances for the Gaussian and impulsive components, which agrees with the assumption of unequal Gaussian factors for the MCA model.

Acknowledgment

This work was funded by the German Research Foundation (DFG). We further gratefully acknowledge support by Hella GmbH and Klöckner Desma GmbH.

References

[1] K. L. Blackard, T. S. Rappaport, and C. W. Bostian, "Measurements and models of radio frequency impulsive noise for indoor wireless communications," *IEEE Journal on Selected Areas in Communications*, vol. 11, no. 7, pp. 991–1001, Sep 1993.

[2] M. Nassar, K. Gulati, M. DeYoung, B. Evans, and K. Tinsley, "Mitigating near-field interference in laptop embedded wireless transceivers," *IEEE International Conference on Acoustics, Speech and Signal Processing*, pp. 1405–1408, March 2008.

[3] S. Bhatti, I. A. Glover, R. Atkinson, P. J. Moore, I. E. Portugues, and R. Rutherford, "Noise amplitude distribution of impulsive noise from measurements in a power substation," in *International Universities Power Engineering Conference (UPEC 2009)*, Sept 2009, pp. 1–5.

[4] D. Middleton, "Statistical-physical models of electromagnetic interference," *IEEE Transactions on Electromagnetic Compatiability*, vol. EMC-19, no. 3, pp. 106–127, August 1977.

[5] K. McDonald and R. Blum, "A physically-based impulsive noise model for array observations," *Conference Record of the Thirty-First Asilomar Conference on Signals, Systems & Computers*, vol. 1, pp. 448–452, November 1997.

[6] P. Gao and C. Tepedelenlioglu, "Space-time coding over fading channels with impulsive noise," *IEEE Transactions on Wireless Communications*, vol. 6, no. 1, pp. 220–229, January 2007.

[7] L. Berry, "Understanding Middleton's canonical formula for Class-A noise," *IEEE Transactions on Electromagnetic Compatiability*, vol. EMC-23, no. 4, pp. 337–344, november 1981.

[8] T. Shongwe, A. J. H. Vinck, and H. C. Ferreira, "A study on impulse noise and its models," *SAIEE Africa Research Journal*, vol. 106, no. 3, pp. 119–131, 2015.

[9] D. Andrews and C. Mallows, "Scale mixtures of normal distributions," *Journal of the Royal Statistical Society, Series B*, vol. B-36, pp. 99–102, 1974.

[10] S. Rappaport and L. Kurz, "An optimal nonlinear detector for digital data transmission through non-Gaussian channels," *IEEE Transactions on Communication Technology*, vol. 14, no. 3, pp. 266–274, June 1966.

[11] K. A. Saaifan and W. Henkel, "A receiver design for MIMO systems over rayleigh fading channels with correlated impulse noise," in *IEEE Global Communications Conference (GLOBECOM)*, Dec 2012, pp. 2481–2486.